

# Hydroxo Hydrido Complexes of Iron and Cobalt (Sn–Fe–Sn, Sn–Co–Sn): Probing Agostic Sn···H–M Interactions in Solution and in the Solid State

Jörg J. Schneider,<sup>[a]\*</sup> Jörg Hagen,<sup>[a]</sup> Norbert Czap,<sup>[a]</sup> Carl Krüger,<sup>[b]</sup> Sax A. Mason,<sup>[c]</sup> Robert Bau,<sup>[d]</sup> Jürgen Ensling,<sup>[e]</sup> Philipp Gütlich,<sup>[e]</sup> and Bernd Wrackmeyer<sup>[f]</sup>

**Abstract:** Bis(toluene)iron **9** reacts with Lappert's stannylene [Sn{CH(SiMe<sub>3</sub>)<sub>2</sub>]<sub>2</sub>] (**4**) to form the paramagnetic bis-stannylene complex [( $\eta^6$ -toluene)Fe–Sn[CH(SiMe<sub>3</sub>)<sub>2</sub>]<sub>2</sub>] (**10**). Compound **10** reacts with H<sub>2</sub>O to form the hydroxo hydrido complex [( $\eta^6$ -C<sub>7</sub>H<sub>8</sub>)( $\mu$ -OH)(H)–Fe–{Sn[CH(SiMe<sub>3</sub>)<sub>2</sub>]<sub>2</sub>}] (**12**) in high yield; its solid-state structure has been elucidated by X-ray and neutron diffraction analysis. In agreement with the <sup>1</sup>H NMR results, **12** contains a hydridic ligand whose exact coordination geometry could be determined by neutron diffraction. The <sup>1</sup>H and <sup>119</sup>Sn NMR analysis of **12** suggested a multicenter Sn/Sn/H/Fe bonding interaction in solution, based on significantly large values of  $J(\text{Sn}, \text{H}, \text{Fe}) = 640 \pm 30$  Hz and  $J(^{119}\text{Sn}, ^{119}\text{Sn}) = 4340 \pm 100$  Hz. In solution, complex **12** exists as two diaster-

eomers in a ratio of about 2:1. Neutron diffraction analysis has characterized **12** as a classical metal hydride complex with very little Sn···H interaction and a typical Fe–H single bond (1.575(8) Å). This conclusion is based on the fact that the values of the Sn···H contact distances (2.482(9) and 2.499(9) Å) are not consistent with strong Fe–H···Sn interactions. This finding is discussed in relation to other compounds containing M–H···Sn units with and without strong three-center interactions. The neutron diffraction analysis of **12** represents the first determination of a Sn–H atomic distance employing this analytical technique. The cobalt analogues [( $\eta^5$ -Cp)( $\mu$ -

OH)(H)Co–{Sn[CH(SiMe<sub>3</sub>)<sub>2</sub>]<sub>2</sub>}] (**15**) and [( $\eta^5$ -Cp)(OD)(D)Co–{Sn[CH(SiMe<sub>3</sub>)<sub>2</sub>]<sub>2</sub>}] [**D**<sub>2</sub>]**15**, which are isolobal with **12**, were prepared by the reaction of [( $\eta^5$ -Cp)Co–Sn{CH(SiMe<sub>3</sub>)<sub>2</sub>]<sub>2</sub>] (**14**) with H<sub>2</sub>O and D<sub>2</sub>O, respectively. The magnitude of  $J(\text{Sn}, \text{H})$  (539 Hz) in **15** is in the same range as that found for **12**. The molecular structure of **15** has been determined by X-ray diffraction which reveals it to be isostructural with **12**. The coordination geometries of the Co(Fe)–Sn1–O–Sn2 arrangements in **12** and **15** are fully planar within experimental error. Compounds **10** and **15** are rare examples of fully characterized complexes obtained as primary products from water activation reactions.

**Keywords:** cobalt • iron • metal hydrides • stannylenes • tin

## Introduction

Stannylenes or stannanediyls are intriguing ligands with respect to structure, bonding, and their capability to coordinate to bare transition metals or transition metal fragments.<sup>[1]</sup> They have played an important role in the search for stable multiply bonded main group organometallic compounds. Homonuclear multiple bonding in heavier main group elements was established for the first time in the landmark compound [Sn{CH(SiMe<sub>3</sub>)<sub>2</sub>]<sub>2</sub>] (**4**), which represents the prototype of such a molecule and was synthesized by Lappert and co-workers as early as 1973.<sup>[1a]</sup>

Heavier main group carbene analogues of tin of general formula :SnR<sub>2</sub> can be subdivided into two classes: base-stabilized and nonbase-stabilized stannylenes (so-called “bis-hydrocarbyl or silyl-substituted stannylenes”)<sup>[2]</sup> (Figure 1).

For the group of base-stabilized stannylenes, various alkyl-substituted compounds of Group 15 elements are able to

[a] Priv.-Doz. Dr. J. J. Schneider, Dr. J. Hagen, Dr. N. Czap

Institut für Anorganische Chemie der Universität  
Universitätsstrasse 5-7, 45117 Essen (Germany)

Fax: (+49) 208-306-4195

E-mail: joerg.schneider@uni-essen.de

[b] Prof. Dr. C. Krüger

Max-Planck-Institut für Kohlenforschung  
45470 Mülheim an der Ruhr (Germany)

[c] Dr. S. A. Mason

Institute Max von Laue-Paul Langevin  
38042 Grenoble Cedex 9 (France)

[d] Prof. Dr. R. Bau

Department of Chemistry, University of Southern California  
Los Angeles, CA 90089 (USA)

[e] Dr. J. Ensling, Prof. Dr. P. Gütlich

Institut für Anorganische und Analytische Chemie Johannes-Gutenberg-Universität Mainz, 55099 Mainz (Germany)

[f] Prof. Dr. B. Wrackmeyer

Laboratorium für Anorganische Chemie  
Universität Bayreuth, 95440 Bayreuth (Germany)

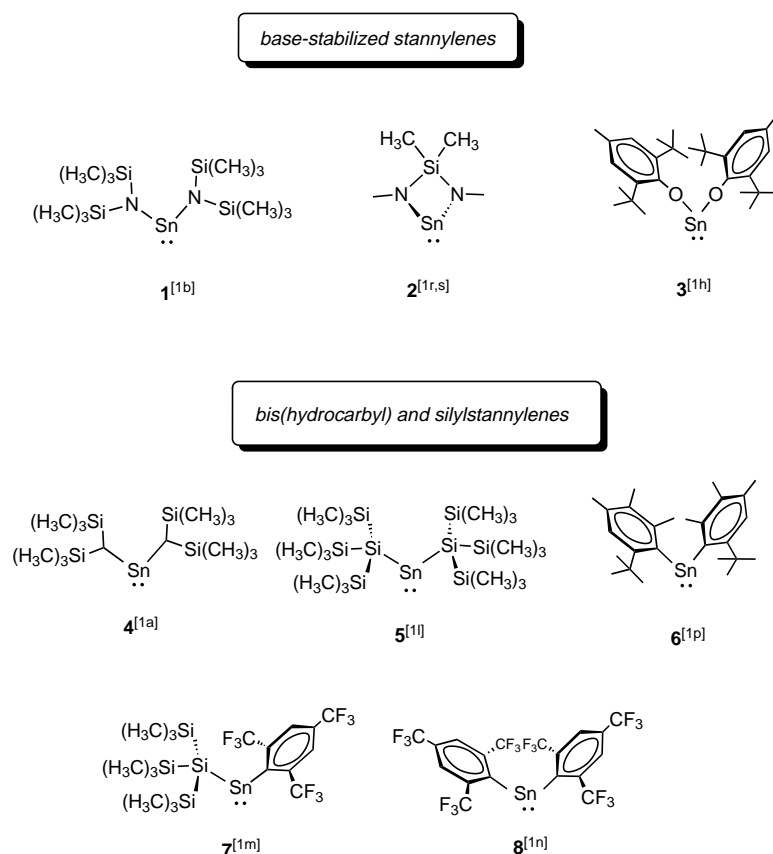


Figure 1. Examples of base-stabilized and bis(hydrocarbyl) and silylstannylenes  $:\text{SnR}_2$ .

influence the divalent  $\text{Sn}^{\text{II}}$  center electronically as donor ligands, and thus the reactivity of these stannylenes can be tuned over a wide range. In contrast, for the group of hydrocarbyl-substituted stannylenes, of which **4** is the most prominent, bulky alkyl or aryl ligands stabilize the subvalent  $\text{Sn}^{\text{II}}$  center mainly kinetically, thus allowing a different course of reactivity compared with their base-stabilized counterparts. For both groups it is noteworthy that their chemistry is usually consistent with a monomeric stannanedyl formulation seen for compounds that are monomeric in solution such as  $[\text{Sn}\{\text{CH}(\text{SiMe}_3)_2\}_2]$  (**4**)<sup>[1a, u]</sup> or  $[\text{Sn}(\text{HC}_6\text{-}2,3,4\text{-tri-methyl-}6\text{-}i\text{Bu})_2]$  (**6**).<sup>[1p]</sup> Organotransition metal complexes in which more than one  $\text{SnR}_2$  fragment is bonded to a single transition metal are, however, still rare for all classes—base-stabilized or bis-hydrocarbyl and silyl stannylenes.

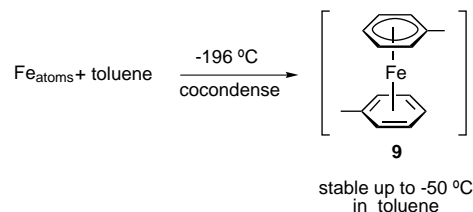
In recent work it has been shown that base-free stannylenes, especially Lappert's  $[\text{Sn}\{\text{CH}(\text{SiMe}_3)_2\}_2]$  (**4**), behave as ligands to low-valent metal fragments.<sup>[1]</sup> These studies have proven that **4** can coordinate to low-valent organonickel, -palladium, -platinum, -cobalt, and -iron fragments. Furthermore, the resulting complexes containing  $\text{Sn-M}$  bonds are reactive towards the insertion of main group elements as well as towards organic molecules.<sup>[1, 3, 4]</sup>

Here we describe the synthesis and structure determination of the first hydroxo hydrido cobalt and iron bis-stannylene compounds derived from Lappert's stannylene **4** and mono-metallic cobalt and iron organometallic complexes. To the best of our knowledge, these complexes represent the first fully characterized examples of such compounds in the iron

metal triad (Fe, Co, Ni) and are rare cases of primary reaction products derived from such reactions with  $\text{H}_2\text{O}$ . Aside from a general interest in structure and bonding of hydrido hydroxo complexes, there is a tremendous interest in compounds able to activate water or alcohol by oxidative addition reactions under mild conditions. Such complexes have been postulated quite frequently as intermediates or transition states in catalytic hydrogenations of carbonyl compounds.<sup>[5]</sup> However, structurally characterized examples of water-activation processes are scarce so far.<sup>[5a, e, 6]</sup> Since metal complexes containing both a hydride and a  $:\text{SnR}_2$  stannylenelike ligand may play an important role in hydrostannylation and related reactions,<sup>[7]</sup> we address the question of the existence of agostic  $\text{Sn}\cdots\text{H-Fe}$  and  $\text{Sn}\cdots\text{H-Co}$  interactions in such complexes in solution and in the solid state by means of NMR and X-ray and neutron diffraction studies.

## Results and Discussion

**Reaction of  $[\text{Sn}\{\text{CH}(\text{SiMe}_3)_2\}_2]$  (**4**) with the Fe atom/toluene solvate complex **9**:** Cryogenic cocondensation of iron atoms and toluene at  $-196^\circ\text{C}$  followed by subsequent work-up at  $-78^\circ\text{C}$  affords a stable, deep brown solution of toluene-solvated iron atoms containing complex **9** as the sole product (Scheme 1). Such a solution represents a most useful source of

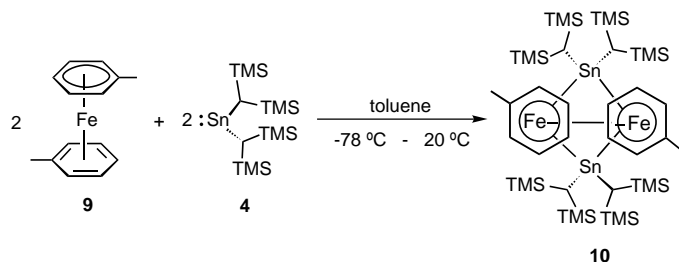


Scheme 1. Formation of bis(toluene)iron **9**.

zerovalent iron for which the name “solvated iron atoms” has been coined.<sup>[8]</sup> Even though the discrete structure of **9** is not known, it is believed to have a characteristic sandwich structure with one toluene ligand  $\eta^6$ -bonded and the other one probably  $\eta^4$ -bonded.<sup>[9]</sup> Careful preparation and isolation techniques allow arene solutions of **9** to be stored and handled by standard Schlenk techniques, which makes them valuable and highly reactive sources for  $\{(\eta^6\text{-toluene})\text{Fe}\}$  fragments in a

“bottled” form for stoichiometric organometallic reactions. Thus complex **9** is the ultimate precursor for the introduction of these metal ligand fragments.

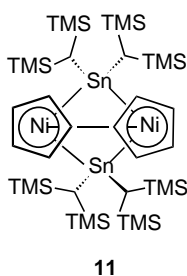
An aliquot of a solution of **9** in toluene (0.025 M) was allowed to react with a twofold molar ratio of **4** dissolved in toluene over a temperature range from  $-78^{\circ}\text{C}$  to room temperature. As the reaction mixture was slowly warmed to room temperature, the color of the resulting solution changed from brown to green. Evaporation of all the volatile components at room temperature gave a brown oil which was recrystallized from diethyl ether to give a greenish brown microcrystalline solid **10** (Scheme 2).



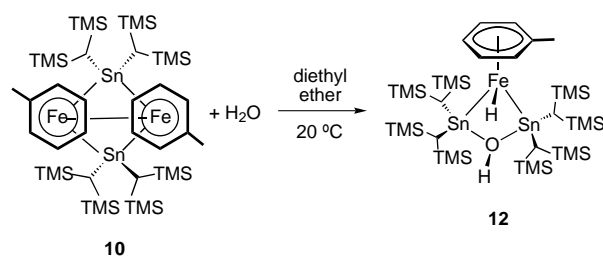
Scheme 2. Synthesis of the bis-stannylene complex **10**. TMS = trimethylsilyl.

The typical reactivity pattern for **9** is the easy loss of its  $\eta^4$ -bonded toluene ligand to yield reactive  $14\text{ e } \{(\eta^6\text{-toluene})\text{Fe}\}$  fragments. These can be intercepted and stabilized by various organic ligands to give monometallic, bimetallic, and cluster products.<sup>[10]</sup> Based on these findings, the substitution of the  $\eta^4$ -bonded toluene moiety of **9** by  $2\text{ e } \text{SnR}_2$  fragments offers a straightforward approach and the most realistic reaction pathway to compound **10**.

Recently we have reported the synthesis and structure of a dinuclear Ni stannylene complex **11** with a  $\text{Ni}_2\text{Sn}_2$  butterfly arrangement and a Ni–Ni bond.<sup>[11]</sup> Compound **10** is two electrons short of the overall electron count of the  $\text{Ni}_2\text{Sn}_2$  cluster **11**, which is known to react with  $\text{H}_2\text{O}$  to give a  $\mu$ -hydroxo-bridged compound.<sup>[9]</sup>

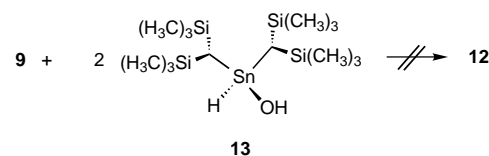


**Reaction of **10** with  $\text{H}_2\text{O}$ :** Because of the unsaturated nature of **10**, reactivity analogous to that of **11** might be expected. Indeed, addition of an excess of water saturated with  $\text{N}_2$  to a greenish brown solution of **10** in toluene results in a color change to bright red after 30 min of stirring. Evaporation of all the volatile components and work-up by crystallization affords bright red, brick-shaped crystals of the hydroxo hydrido compound **12** (Scheme 3), which are stable in air



Scheme 3. Formation of the hydroxo hydrido complex **12**. TMS = trimethylsilyl.

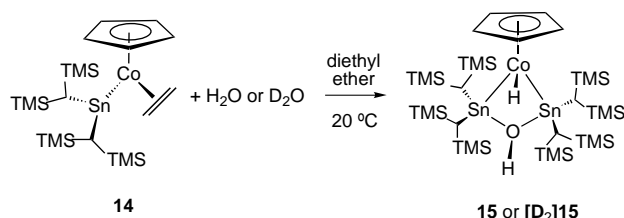
for several hours. Compound **12** was also obtained by chromatography of a solution of **10** in toluene on  $\text{Al}_2\text{O}_3$  containing less than 1%  $\text{H}_2\text{O}$ . However, chromatography on freshly dried  $\text{Al}_2\text{O}_3$ , containing virtually no water, leaves **10** unchanged, clearly indicating the high reactivity of the iron–tin complex **10** towards nucleophilic attack by trace amounts of water. This observation for **10** is in accord with the fact that the dinuclear Ni complex **11** displays the same reactivity towards  $\text{H}_2\text{O}$ .<sup>[11]</sup> To the best of our knowledge, this result describes the first case of water activation across an iron–tin bond. Recent reports by Pörschke and co-workers describe reversible water and alcohol activation across the Pd–Sn bond in  $[(i\text{PrPCH}_2\text{CH}_2\text{P}i\text{Pr}_2)\text{Pd} - \text{Sn}\{\text{CH}(\text{SiMe}_3)_2\}_2]$ .<sup>[12]</sup> Our attempts to eliminate water reversibly from **12** have not been successful so far and have resulted in decomposition of **12**. The initial step of water activation by compound **10** to give **12** might involve attack of the M–M bond in **10**. This is substantiated by the fact that the hydroxo hydrido diorganostannane **13**,<sup>[13]</sup> containing  $\text{H}_2\text{O}$  in a “preactivated” form, does not react with the monometallic organoiron compound **9** to give **12**. Reaction of compound **13** with **9** at  $-78^{\circ}\text{C}$  followed by subsequent warming to room temperature leads only to decomposition of **9** into metallic iron and toluene, but leaves **13** unchanged (Scheme 4). This indicates that **9**, containing tetravalent tin, is unreactive towards low-valent  $14\text{ e } (\eta^6\text{-toluene})\text{Fe}$  fragments.



Scheme 4. Reaction of complex **9** with the hydroxo hydrido stannane **13**.

**Reaction of  $[(\eta^5\text{-Cp})(\eta^2\text{-ethene})\text{Co} - \text{Sn}\{\text{CH}(\text{SiMe}_3)_2\}_2]$  (**14**) with  $\text{H}_2\text{O}$  and  $\text{D}_2\text{O}$ :** Experimental support of initial attack of water either at the Fe–Fe bond of **10** or at one of the individual Fe centers comes from the reactivity of the mono(ethene)(stannylene)cobalt complex **14** towards  $\text{H}_2\text{O}$  or  $\text{D}_2\text{O}$ , which we have also studied. Recently we reported the high reactivity of **14** towards insertion and addition reactions of the unbridged low-coordinated Co–Sn bond.<sup>[4b]</sup> Characteristic of the unusual reactivity of **14** is the easy loss of ethene which generates a coordinatively and electronically highly reactive  $16\text{ e}$  organocobalt/tin fragment that is formed upon ethene loss in all reactions observed for **14** so far. Addition of

an excess of nitrogen-saturated H<sub>2</sub>O or D<sub>2</sub>O to a solution of **14** in diethyl ether leads initially to evolution of gas and a change in the color from purple to bright red. Work-up and crystallization result in the formation of the thermally stable hydroxo hydrido complex **15** or its deuterium analogue [D<sub>2</sub>]**15** as bright red crystals in 60% or 53% yields, respectively (Scheme 5). Complexes **15** and [D<sub>2</sub>]**15** are isolobal with the hydroxo hydrido iron compound **12**.



Scheme 5. Reaction of water with the (ethene)stannylene complex **14**.

### Spectroscopic characterization:

Complex **10** gave no molecular ion in the electron-impact mass spectrum (EI-MS). The <sup>1</sup>H NMR (27 °C) spectrum of **10** reveals broad signals at  $\delta = 59.7$  (1H), 54.2 (2H), 26.3 (2H), 3.26 (3H), and 1.08 (36H)—highly characteristic for a paramagnetic compound for which large isotropic Fermi contact shifts (as observed for **10**) have been reported.<sup>[14, 15]</sup> This experimental observation is in accord with a dinuclear structure for **10** and a formal electron count of 17 at each Fe<sup>II</sup> center.

The molecular structure of the hydroxo hydrido complexes **12** and **15** can be deduced from their characteristic spectroscopic data. In the EI-MS the molecular ion of **15** is observed with the correct isotopic pattern for the nominal composition C<sub>33</sub>H<sub>83</sub>Co<sub>1</sub>O<sub>1</sub>Si<sub>8</sub>Sn<sub>2</sub>.

In the EI-MS of **12**, in contrast to **15**, no molecular peak arising from [12]<sup>+</sup> is observed, however, characteristic fragments can be detected that indicate subsequent loss of toluene and trimethylsilyl groups from [12]<sup>+</sup>.

The IR spectra (KBr) of **12** and **15** display  $\nu(\text{Sn}-\text{OH}-\text{Sn})$  stretching vibrations at 3650 (**12**) and 3615 cm<sup>-1</sup> (**15**). The isotopomer ([D<sub>2</sub>]**15**) has a  $\nu(\text{OD})$  stretch at 2669 cm<sup>-1</sup>. These frequencies are in accord with the  $\nu(\text{Sn}-\text{OH}-\text{Sn})$  stretching frequencies of the Ni complex [( $\eta^5$ -Cp)Ni{(SiMe<sub>3</sub>)<sub>2</sub>CH}<sub>2</sub>Sn(OH)Sn{CH(SiMe<sub>3</sub>)<sub>2</sub>}<sub>2</sub>]<sup>[11]</sup> ( $\nu(\text{OH})$  3621 cm<sup>-1</sup>) and the hydroxo organostannane complex **13** ( $\nu(\text{OH})$  3660 cm<sup>-1</sup>).<sup>[13]</sup> The bands from the  $\nu(\text{Fe}-\text{H})$  and  $\nu(\text{Co}-\text{H})$  stretching modes in **12** and **15** are unfortunately broad and thus ill-defined, making a reliable assignment impossible.

The <sup>1</sup>H NMR resonances of the  $\eta^6$ -coordinated toluene ligand in the diamagnetic complex **12** are characteristic and in line with other half-sandwich complexes of iron with  $\eta^6$ -bonded toluene ligands (Table 1). The Cp resonance for **15** appears at  $\delta = 4.67$ ; the resonances of the bridging  $\mu$ -hydroxo proton of the Sn–OH–Sn group are found at  $\delta = 1.70$  for **12** and 1.63 for **15** and are in good agreement with the <sup>1</sup>H NMR shift of the terminal Sn–OH resonance in **13** ( $\delta = 1.63$ ).<sup>[13]</sup>

A priori, both CH(SiMe<sub>3</sub>)<sub>2</sub> ligands at each tetracoordinated Sn center in **12** and **15** are enantiotopic, whereas the TMS

Table 1.

Ligand fragment	<sup>1</sup> H NMR (27 °C) $\delta$ (ppm)	Compound	Ref.
$\eta^6$ -toluene toluene-CH <sub>3</sub>	5.06, 4.28, 4.12 1.84	[( $\eta^6$ -toluene)( $\eta^2$ -ethene) <sub>2</sub> iron]	16
$\eta^6$ -toluene toluene-CH <sub>3</sub>	4.92, 4.86, 4.72 1.95	[( $\eta^6$ -toluene)(1,3-cod)iron]	15
$\eta^6$ -toluene toluene-CH <sub>3</sub>	5.35, 4.83, 4.73 2.30	[( $\eta^6$ -toluene){P(OEt) <sub>3</sub> } <sub>2</sub> iron]	15
$\eta^6$ -toluene toluene-CH <sub>3</sub>	5.19, 5.09, 4.71 1.46	[( $\eta^6$ -toluene)(H) <sub>2</sub> Fe{SiCl <sub>3</sub> } <sub>2</sub> ]	19
$\eta^6$ -toluene toluene-CH <sub>3</sub>	4.93, 4.87, 4.49 1.40	[( $\eta^6$ -toluene)(H) <sub>2</sub> Fe{SiF <sub>3</sub> } <sub>2</sub> ]	18
$\eta^6$ -toluene toluene-CH <sub>3</sub>	5.51, 5.38, 4.55 2.31	[( $\eta^6$ -toluene)(OH)(H)Fe- {Sn{CH(SiMe <sub>3</sub> ) <sub>2</sub> } <sub>2</sub> }] <b>12</b>	this work
$\eta^6$ -toluene toluene-CH <sub>3</sub>	5.37, 5.13, 4.54 1.83	[( $\eta^6$ -toluene)-Fe] <sub>2</sub> $\mu_2$ -{ $\eta^3$ - $\eta^3$ -toluene}]	14

groups of each SnR<sub>2</sub> substituent are diastereotopic. In the <sup>13</sup>C NMR spectrum, one resonance for the CH(SiMe<sub>3</sub>)<sub>2</sub> carbons and two resonances for the carbons of the TMS substituents at each SnR<sub>2</sub> ligand fragment are observed. This tallies with the existence of a mirror plane that renders the individual CH(SiMe<sub>3</sub>)<sub>2</sub> substituents on each SnR<sub>2</sub> fragment equivalent and gives rise to the observation of four TMS signals and two CH(SiMe<sub>3</sub>)<sub>2</sub> resonances for both SnR<sub>2</sub> ligands in **12**. For **15** the same explanation holds true, but an incomplete set of <sup>13</sup>C resonances is observed, probably because of an isochronicity of the relevant positions (see Experimental Section).

Additional <sup>1</sup>H NMR signals at high field are observed for **12** (−13.4) and **15** (−17.5) and are indicative of Fe–H and Co–H groups. The hydride resonances in the related half-sandwich complexes bis(trifluorosilyl)- or bis(trichlorosilyl)( $\eta^6$ -toluene)iron(dihydride) at  $\delta = -19$  (SiF<sub>3</sub>) and −17.15 (SiCl<sub>3</sub>) are shifted nearly 6 ppm upfield from that of **12**.<sup>[19, 20]</sup> The hydride signals for **12** and **15** are accompanied by <sup>119</sup>Sn satellites (with intensities for two tin atoms in each complex) that correspond to a rather large magnitude of <sup>2</sup>J(Sn,H), which suggests the existence of three-center Fe,H,Sn and Co,H,Sn interactions, respectively. J(Si,H) coupling constants have often been used as a criterion for the presence of Si–H–M contacts.<sup>[21]</sup> The same is true for the analogous J(Sn,H) data in transition metal tin hydrides, which have been recognized as a valuable analytical tool to gauge the presence of agostic M–H⋯Sn interactions. The magnitude of the coupling constants correlates with the amount of Sn⋯H interaction. At one extreme are the values for Sn–H interactions in tetrahedral alkyltin hydrides with direct Sn–H  $\sigma$ -bonding. Their <sup>1</sup>J(Sn,H) values are typically in the upper region (1500–2000 Hz<sup>[22]</sup>), as exemplified by the Sn<sup>IV</sup> compound **11** (<sup>1</sup>J(Sn,H) = 1991 Hz).<sup>[13]</sup> At the other extreme, J(Sn,H) coupling constants distinctively below 150 Hz are characteristic for compounds without any three-center Sn,H,M bonding. The intermediate range between 150–300 Hz is distinctive of compounds exhibiting three-center Sn,H,M interactions with a varying degree of Sn,H,M contact defined by the relative size of the coupling constant. In **12** and **15**, the J(Sn,H) couplings are 630

(**12**) and 593 Hz (**15**), respectively, and these values point towards the presence of  $\eta^2$ -Sn–H–Fe(Co) interactions in solution. The  $J(\text{Sn},\text{H})$  values in **12** and **15** are significantly larger than those found in the manganese, chromium, and iron compounds  $[(\eta^5\text{-MeC}_5\text{H}_4)(\text{CO})_2\text{Mn}(\text{H})\text{SnPh}_3]^{[23]}$  (270 Hz),  $[(\eta^6\text{-Mes})\text{Cr}(\text{CO})_2(\text{H})\text{SnPh}_3]^{[24]}$  (327.6 Hz), and  $[\text{FeH}_3(\text{P-Ph}_2\text{Et})_3\text{SnPh}_3]^{[25]}$  (174.2 Hz) synthesized by Schubert et al., as well as in  $[\eta^6\text{-1,4-C}_6\text{H}_4(\text{OCH}_3)_2\text{Cr}(\text{CO})_2(\text{HSnPh}_3)]^{[26]}$  (213.60 for  $^{119}\text{Sn}$  and 208.0 Hz for  $^{117}\text{Sn}$ ) prepared by Klabunde et al. The Mn and Cr complexes prepared by Schubert et al. and the Cr complex prepared by Klabunde et al. contain definite Sn–H–M three-center interactions based on both NMR and X-ray crystallographic data. In contrast to these typically large values for  $J(\text{Sn},\text{H},\text{M})$  coupling constants, the values for  $J(\text{H},\text{Sn})$  coupling constants without three-center Sn $\cdots$ H–M interactions are 5.3, 8.4, and 15.8 Hz in a series of compounds of the type  $[(\text{Cp})\text{Fe}(\text{H})(\text{CO})\text{Sn}(\text{R}_3)_2]$  (R = Me, Bu, Ph);<sup>[27]</sup> or are between 15 and 45 Hz in  $[(i\text{PrPCH}_2\text{CH}_2\text{P}i\text{Pr}_2)\text{Pd-Sn}[\text{CH}(\text{SiMe}_3)_2]_2]^{[12]}$  or as low as 23.7 Hz in  $[(\text{Cp})\text{Cr}(\text{NO})(\text{PPh}_3)(\text{H})\text{SnPh}_3]^{[28]}$ . In those complexes, as judged from the magnitude of their  $^2J(\text{Sn},\text{H})$  coupling, any chemical bonding interaction between Sn and H seems to be negligible.<sup>[29]</sup>

An interesting case is represented by  $[\text{Cp}_2\text{Mo}(\text{H})\text{SnR}_3]$  ( $\text{R}_3 = \text{Me}_3, \text{Me}_2\text{Cl}$ )<sup>[30]</sup> because it is completely opposite to the observations discussed above, as these compounds have large  $^2J(\text{Sn},\text{H})$  values of 310 and 238 Hz, respectively, which are indicative of a distinct three-center Sn $\cdots$ H–Mo interaction in solution. However, the corresponding X-ray analysis revealed *no* such interaction in the solid state.<sup>[30]</sup> The same situation has been found for  $[\text{FeH}_3(\text{PPh}_2\text{Et})\text{SnPh}_3]^{[25]}$  whose metal skeleton shows an approximate  $C_3$  symmetry in the crystalline state and a nearly tetrahedral  $\text{FeP}_3\text{Sn}$  core. Although the relevant hydrogen positions in  $[\text{FeH}_3(\text{PPh}_2\text{Et})\text{SnPh}_3]$  could not be located by X-ray structure analysis, its NMR spectrum was interpreted in terms of the presence of a Sn–H–Fe three-center, two-electron interaction based on a large  $^2J(\text{Sn},\text{H})$  coupling constant.<sup>[25]</sup>

In the  $^{29}\text{Si}$  NMR spectrum of **12**, one observes two broad singlets at  $\delta = -0.36$  and  $-1.03$  in a ratio of about 1:2. The  $^1\text{H}$  and  $^{13}\text{C}$  NMR signals of the  $\text{Me}_3\text{Si}$  group are also split into at least three different signals (three for **15**, four for **12**), which points to the presence of diastereomers. The  $^{119}\text{Sn}$  NMR spectrum of **12** in solution shows three fairly broad signals as doublets at  $\delta = 326, 347.5$ , and  $371$  from  $^{119}\text{Sn}$ – $^1\text{H}$  coupling in agreement with the  $^1\text{H}$  NMR spectrum. Two of these signals are accompanied by  $^{117/119}\text{Sn}$  satellites as AX and AB spin systems, respectively (confirmed also by simulated spectra), and the third signal at highest frequency has only  $^{117}\text{Sn}$  satellites. The three signals belong to two diastereomers in which the more abundant (about 66%) has two different tin sites, and the less abundant one (about 33%) has only one tin site. The observation of these diastereoisomers in solution might be due to the different configurations of the  $[\text{CH}(\text{TMS})_2]$  ligands at each tin, which would give rise to the presence of geometrical isomers in a different ratio. The large magnitude of  $|J(^{119}\text{Sn}(1), ^{119}\text{Sn}(2))| = 4370 \pm 100$  Hz points towards marked tin–tin bonding interactions. The description of the bonding situation between Sn(1), Sn(2), Fe,

and H becomes exceedingly complex, possibly invoking fast dynamic processes in solution. In solution a reasonable scenario might be an interchange between different hydride coordination sites (“see-saw” mechanism), which creates a time-averaged hydride position that places the hydride ligand close to the Fe and both Sn atoms (Figure 2). The  $\delta(^{119}\text{Sn})$  values of **12** at rather low field are difficult to interpret in the light of the other evidence. However, it is known that  $^{119}\text{Sn}$  nuclei become markedly deshielded near an oxonium-type oxygen atom.<sup>[31]</sup>

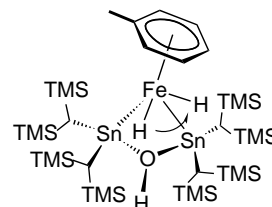


Figure 2. Hydridic ligand interchange in complex **12** by a “see-saw” mechanism.

In summary, all these findings show that there is often conflicting evidence in characterizing three- or multicenter Sn–H–M interactions in solution (by NMR spectroscopy) and in the solid state (by X-ray crystallography). Despite the fact that a number of useful X-ray crystallographic studies have been carried out, the hydrogen could only be located with an inherent and systematic uncertainty. Thus far, no three-center Sn,H,M interaction has been further substantiated by other spectroscopic techniques such as solid-state  $^{119}\text{Sn}$  NMR spectroscopy or even neutron diffraction analysis.

### Structural investigations:

**X-ray studies**<sup>[32]</sup> of **12** and **15**: The molecular structures of **12** and **15** in the solid state were determined by X-ray crystallography (Figures 3 and 4, respectively). In both compounds the

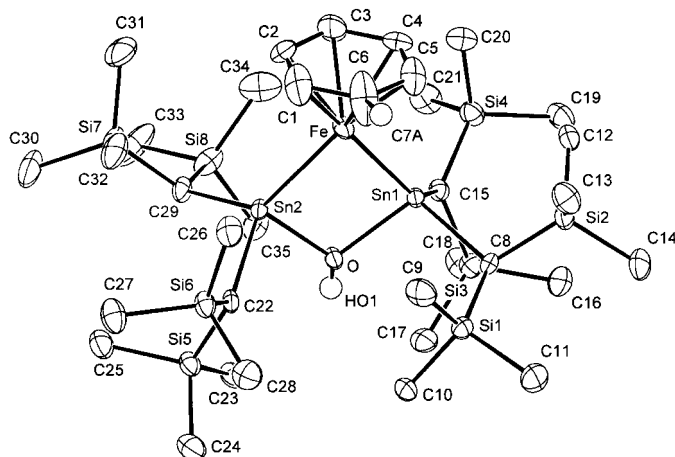


Figure 3. Molecular structure of **12** (ORTEP) in the solid state as determined by X-ray diffraction. Selected bond lengths [Å] and angles [°]: Sn1–Fe 2.525(1), Sn1–O 2.139(3), Sn1–C(8) 2.213(4), Sn1–C15 2.219(3), Sn2–Fe 2.525(1), Sn2–O 2.147(3), Sn2–C22 2.234(5), Sn2–C29 2.215(5), O–HO1 0.69(5); C15–Sn1–C8 105.5(2), C15–Sn1–O 90.7(1), C15–Sn1–Fe 129.8(1), C8–Sn1–O 104.3(1), C8–Sn1–Fe 122.9(1), O–Sn1–Fe 89.6(1), C29–Sn2–C22 106.3(2), C29–Sn2–O 103.9(2), C29–Sn2–Fe 124.0(1), C22–Sn2–O 91.1(1), C2–Sn2–Fe 127.9(1), O–Sn2–Fe 89.4(1).

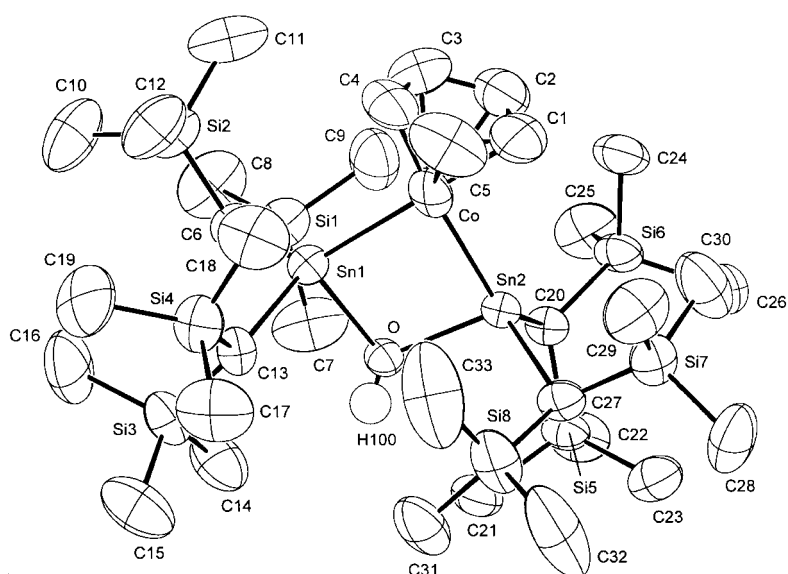


Figure 4. Molecular structure of **15** (ORTEP) in the solid state as determined by X-ray diffraction. Selected bond lengths [Å] and angles [°]: Sn1–Co 2.464(1), Sn2–Co 2.466(1), Sn1–O 2.147(3), Sn2–O 2.158(3), Sn1–C6 2.213(5), Sn1–C13 2.221(3), Sn2–C20 2.220(4), Sn2–C27 2.210(5); C13–Sn1–C6 108.7(2), C27–Sn2–C20 107.0(2), C6–Sn1–Co 121.5(1), C13–Sn1–Co 127.8(1), C6–Sn1–O 105.1(2), O–Sn1–Co 88.3(1), C27–Sn2–O 106.5(2), C27–Sn2–Co 123.0(1), C20–Sn2–O 92.5(2), C20–Sn2–Co 127.7(1), O–Sn2–Co 87.9(1), Sn2–Co–Sn1 83.9(1), Sn2–O–Sn1 99.9(1), H100–O–Sn1 124.1(3), H100–O–Sn2 129.3(3).

two  $\text{SnR}_2$  fragments, the Co and the Fe atoms, and the  $\mu\text{-OH}$  group define a planar cyclic geometrical arrangement (M–Sn–O–Sn). The dihedral angles Co–Sn–O–Sn and Fe–Sn–O–Sn are  $1.35(4)^\circ$  and  $0.32(5)^\circ$ , respectively. The two Sn atoms in **12** and **15** are tetracoordinate, both having a similar strongly distorted “tetrahedral” coordination geometry. As a result, bonding parameters at both  $\text{Sn}^{\text{II}}$  centers in **12** and **15** are comparable. The average Sn–Sn distance is  $3.294 \text{ \AA}$  in **12** and  $3.282 \text{ \AA}$  in **15**, which indicates a weak but significant Sn–Sn bonding interaction for both complexes in good agreement with the Sn NMR results.

The Co–Sn bond lengths in **15** are  $2.464(1)$  and  $2.466(1) \text{ \AA}$  and are significantly shorter than the Fe–Sn bonds in **12** ( $2.525(1) \text{ \AA}$ ) by  $0.06 \text{ \AA}$ . This relative lengthening of the Fe–Sn distances must obviously be attributed to some degree of bonding differences based on electronic grounds, since the steric ligand environments in both isostructural complexes are nearly identical. For both complexes **12** and **15**, the Co–Sn and Fe–Sn bond lengths are significantly elongated when compared with the mono(ethene)(stannylene)(Cp)cobalt **14** ( $2.386 \text{ \AA}$ ) and the corresponding isolobal mono(ethene)-(stannylene)(toluene)iron complex **16**<sup>[4b]</sup> ( $2.4362(10) \text{ \AA}$ ), respectively, each of which contain three-coordinate tin centers.

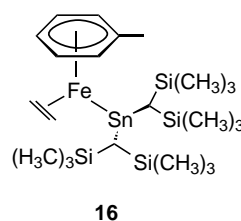


Table 2 gives selected bonding parameters for **15** and the structurally related chalcogen-bridged complexes **17** and **18** containing the heavier element homologues Se and Te in a  $\mu_3$ -bridging mode that connect the two Sn atoms and the central Co atom in a similar fashion to that of the OH group in **15**.

The Fe–Sn bond length in **12** is in the lower region of those observed for a set of nineteen compounds that contain Fe–Sn bonds in the range between  $2.46$  and  $2.67 \text{ \AA}$ .<sup>[1b]</sup> It is noteworthy that the shortest Fe–Sn bond is observed in the bisstannylene complex  $[\text{Fe}(\text{CO})_4\{\text{Sn}(\text{OAr})_2\}_2]$  (Ar =  $\text{C}_6\text{H}_2\text{tBu}_2$ -2,6-Me<sub>4</sub>) (Fe–Sn =  $2.408 \text{ \AA}$ ),<sup>[1b]</sup> well in accord with the extraordinarily good  $\pi$ -donor properties of the base-stabilized stannylene ligand  $\text{Sn}(\text{OAr})_2$ .<sup>[1b]</sup>

**Neutron diffraction analysis of 12:**<sup>[32]</sup> Compounds **12** and **15** both contain hydridic ligands. We have demonstrated that

Table 2. Selected bonding parameters of **15** and for related Co/Se<sup>[4b]</sup> and Co/Te<sup>[4b]</sup> compounds **17** and **18**.<sup>[a]</sup>

angle [°]	<b>15</b>	<b>17</b>	<b>18</b>
Sn1–E–Sn2	100.3	90.90	85.86
C1–Sn1–C8	108.7	109.8	109.5
C15–Sn2–C22	107.0	108.1	106.7

[a] R = trimethylsilyl.

there is evidence of multicenter Sn,Sn,Fe,H bonding in **12** by both  $^1\text{H}$  and  $^{119}\text{Sn}$  NMR in solution, but it was also important to look for such structural features in the solid state. Interestingly, however, there is only one report in which characterization of this type of interaction has been successful in solution *and* in the solid state (by NMR spectroscopy and X-ray diffraction) for a Fe/Sn complex. This gave corresponding results with respect to the existence of a  $\eta^2\text{-Sn-H-M}$  interaction.<sup>[23]</sup> As far as X-ray diffraction as an analytical tool is concerned, determination of hydrogen positions is a procedure with an inherently low degree of accuracy because of the fact that the X-ray diffraction process locates the electron density maximum of a M–H bond and not the actual nuclear positions. Thus, bond lengths and angles involving hydrogen are usually observed to be significantly off their true values when determined by X-ray diffraction.<sup>[33, 34]</sup> However, these problems do not arise with neutron diffraction, which directly locates the nuclear positions of the H atoms. As we were able to obtain sufficiently large crystals of our iron hydride compound **12**, we were eager to determine its solid-state structure by neutron diffraction in order to determine the coordination geometry of the Sn, H, and Fe atoms in the most accurate way.

The molecular plot (ORTEP) of **12** as determined by neutron diffraction is shown in Figure 5. The structural analysis of the compound was complicated by a packing

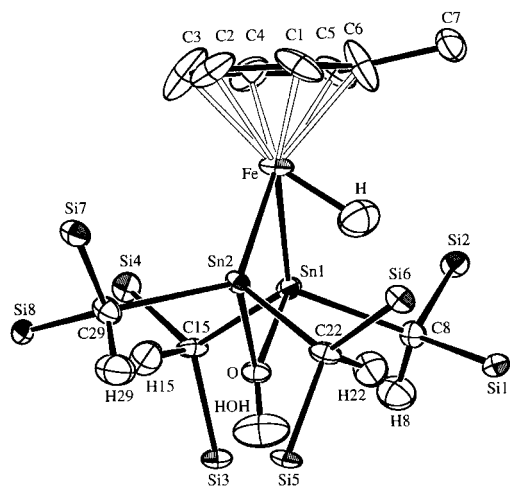
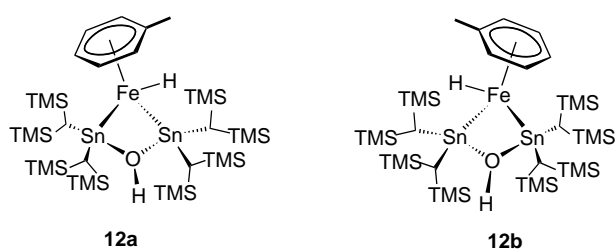


Figure 5. Molecular structure of **12** (ORTEP) in the solid state as determined by neutron diffraction. Only one of the two disordered orientations of the hydride and toluene ligands is shown. The Fe–H distance is 1.581(8) Å, and the Sn $\cdots$ H distances are 2.477(9) Å (minor isomer) and 2.497(9) Å (major isomer), respectively. For selected bond lengths [Å] and angles [°] see Table 4.

disorder of the toluene and hydride ligands, in which 75% of the molecules pack with orientation **12a** and 25% with an



orientation rotated by 180°, **12b**. What is observed experimentally is a superposition of these orientations. The rest of the structure (the Fe–Sn–OH–Sn core and the CH(SiMe<sub>3</sub>)<sub>2</sub> ligands) however is ordered. For the following discussion of the structure only the major hydride H site is considered (Table 3 and 4).

The original motivation for carrying out the neutron diffraction analysis of **12** was to see if evidence for Fe–H $\cdots$ Sn agostic interactions could be found in the solid state, as suggested by NMR results in solution (*vide supra*). The neutron diffraction results show a molecule with essentially a terminal Fe–H bond, with almost no evidence of significant H $\cdots$ Sn interactions in the solid state (Figure 5). The Fe–H

Table 3. Neutron diffraction details of **12**.

empirical formula	C <sub>35</sub> H <sub>85</sub> Fe O Si <sub>8</sub> Sn <sub>2</sub>
<i>T</i> [K]	20(1)
wavelength [Å]	1.5345(1)
space group	monoclinic, <i>P</i> 2 <sub>1</sub> / <i>n</i> (no. 14)
unit cell dimensions	
<i>a</i> [Å]	13.6760(4)
<i>b</i> [Å]	17.6418(6)
<i>c</i> [Å]	23.6655(7)
$\alpha$ [°]	90
$\beta$ [°]	104.000(2)
$\gamma$ [°]	90
<i>V</i> [Å <sup>3</sup> ]	5540.1
<i>Z</i>	4
crystal size [mm]	1.5 × 1.5 × 1.5
$\theta$ range for data collection	3.14° to 50.55°
index ranges	–13 ≤ <i>h</i> ≤ 13, –17 ≤ <i>k</i> ≤ 17, –12 ≤ <i>l</i> ≤ 23
reflections collected	10318
independent reflections	5678 [ <i>R</i> (int) = 0.0362]
data/restraints/parameters	5675/38/1259
Goodness-of-fit on <i>F</i> <sup>2</sup>	0.976
Final <i>R</i> indices [ <i>I</i> > 2( <i>I</i> )]	<i>R</i> ( <i>F</i> ) = 0.0782, <i>R</i> ( <i>wF</i> <sup>2</sup> ) = 0.1800
<i>R</i> indices (all data)	<i>R</i> ( <i>F</i> ) = 0.0910, <i>R</i> ( <i>wF</i> <sup>2</sup> ) = 0.1929

Table 4. Selected bond lengths [Å] and angles [°] for **12** as determined by neutron diffraction.

Fe–H	1.581(8)		
Sn1–Fe	2.519(3)	Sn–Fe	2.514(3)
Sn1 $\cdots$ H	2.477(9)	Sn2 $\cdots$ H	2.497(9)
Sn1–O	2.150(4)	Sn2–O	2.140(4)
Sn1–C8	2.204(4)	Sn2–C22	2.222(4)
Sn1–C15	2.229(4)	Sn2–C29	2.218(4)
Sn1 $\cdots$ Sn2	3.269(4)		
Si1–C8	1.877(5)	Si5–C22	1.891(5)
Si2–C8	1.882(5)	Si6–C22	1.890(5)
Si3–C15	1.887(5)	Si7–C29	1.879(5)
Si4–C15	1.890(5)	Si8–C29	1.875(5)
O–H(OH)	0.938(9)		
C8–H8	1.103(7)	C22–H22	1.097(7)
C15–H15	1.087(7)	C29–H29	1.091(7)
Sn2–Fe–Sn1	81.0(1)		
Sn1–Fe–H	70.1(3)	Sn2–Fe–H	71.0(3)
Fe–H $\cdots$ Sn1	73.3(3)	Fe–H $\cdots$ Sn2	72.5(3)
O–Sn1–Fe	89.6(2)	O–Sn2–Fe	90.0(2)
C8–Sn1–Fe	122.0(2)	C22–Sn2–Fe	126.7(2)
C15–Sn1–Fe	130.6(2)	C29–Sn2–Fe	125.1(2)
O–Sn1–C8	103.9(2)	O–Sn2–C22	90.5(2)
O–Sn1–C15	90.7(2)	O–Sn2–C29	103.4(2)
C8–Sn1–C15	105.7(2)	C29–Sn2–C22	106.5(2)
Sn2–O–Sn1	99.3(2)		
Sn1–O–H(OH)	129.7(5)	Sn2–O–H(OH)	129.6(5)

distance is found to be 1.581(8) Å as would be expected<sup>[35]</sup> for an Fe–H single bond, while the Sn⋯H distances are 2.477(9) and 2.497(9) Å. By comparing these with the estimated values<sup>[36]</sup> of 1.77 Å for an Sn–H single bond and 2.07 Å for the Sn⋯H distance in an agostic Sn⋯H–M interaction, one can conclude that the Sn–H distances we find in **12** are too long for any meaningful Sn–H bonding interaction in the solid state.

As was found in the X-ray analysis, the FeSn<sub>2</sub>O core of the molecule is planar, within experimental error, as is the Sn–OH–Sn group at the three-coordinate O atom of the bridging hydroxyl ligand. The O–H distance of that ligand was found to be 0.938(9) Å, and all the other distances and angles in the structure were also found to be normal.

**Mössbauer spectroscopy:** Assigning formal oxidation states to iron and cobalt as well as to tin in **12** and **15** gives formal charges of +2 for Fe (d<sup>6</sup>) and +3 for Co (d<sup>6</sup>) in accord with their overall diamagnetic NMR behavior. For each of the two tin centers a formal charge of +2.5 results as the two Fe–Sn bonds are formally electronically neutral and the bridging OH ligand contributes a negative charge to the overall electron count of **12** and **15**.

In general, Mössbauer spectroscopy provides valuable experimental information on the authentic valence state (oxidation and spin state) and geometry in coordination compounds. <sup>57</sup>Fe and <sup>119</sup>Sn Mössbauer measurements in zero field were performed on crystalline samples of **12** at 100 and 90 K,<sup>[37]</sup> which gave symmetrically split doublets with isomer shifts of  $\delta_{\text{IS}} = 0.43 \text{ mm s}^{-1}$  (relative to  $\alpha$ -iron) and  $\delta_{\text{IS}} = 1.72 \text{ mm s}^{-1}$ , relative to CaSnO<sub>3</sub>, and quadrupole splittings of  $\Delta E_{\text{Q}} = 0.95$  and  $2.97 \text{ mm s}^{-1}$  for the iron and tin nuclei, respectively (Figures 6 and 7). Both the iron and tin Mössbauer data are in agreement with a pseudooctahedral coordination environment around iron and a pseudotetrahedral arrangement around tin.<sup>[38]</sup> The values for the iron isomer shift and quadrupole splitting are typical values for Fe<sup>II</sup>.<sup>[38, 39, 40]</sup>

Mössbauer data for organometallic tin compounds can be subdivided into those compounds containing Sn<sup>IV</sup> which show typical isomer shifts and quadrupole splittings well below  $2 \text{ mm s}^{-1}$ , and also into those with distinctively higher  $\delta_{\text{IS}}$  values and quadrupole splittings  $\Delta E_{\text{Q}} (\gg 2 \text{ mm s}^{-1})$  such as those of the Group VIII metals. For both groups the classification depends on preparative procedures, such that

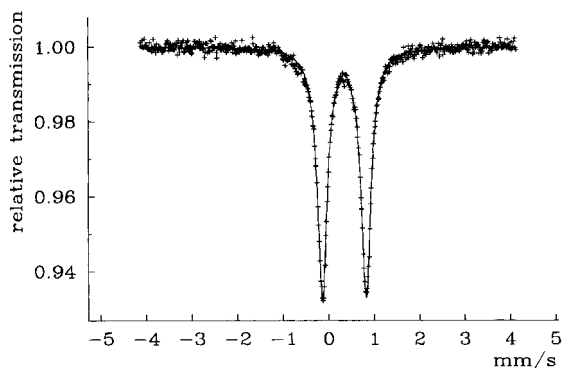


Figure 6. Zero-field <sup>57</sup>Fe Mössbauer spectrum of **12** at 80 K.

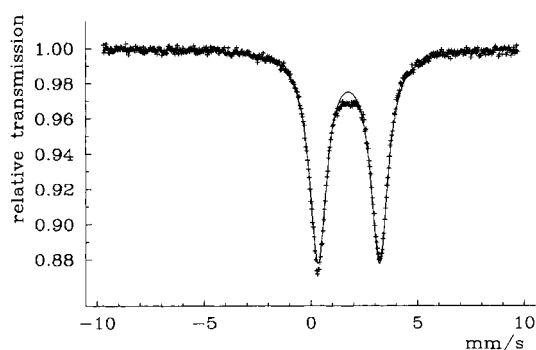


Figure 7. Zero-field <sup>119</sup>Sn Mössbauer spectrum of **12** at 80 K.

compounds assignable to the first class (Mössbauer parameters  $< 2 \text{ mm s}^{-1}$ ) are accessible from SnCl<sub>4</sub>, and those assignable to the second have SnCl<sub>2</sub> as the precursor.<sup>[41]</sup> According to this classification an assignment of **12** ( $\delta_{\text{IS}} = 1.72 \text{ mm s}^{-1}$ ,  $\Delta E_{\text{Q}} = 2.97 \text{ mm s}^{-1}$ ) to one of these two classes is not clear-cut, despite its preparation from the stannylene **4** ( $\delta_{\text{IS}} = 2.16 \text{ mm s}^{-1}$ ;  $\Delta E_{\text{Q}} = 2.31 \text{ mm s}^{-1}$ )<sup>[41b]</sup> that contains a Sn<sup>II</sup> center. In complex **4**, tin has a pseudotetrahedral configuration at each SnR<sub>2</sub> fragment in the solid state. The  $\delta_{\text{IS}}$  values for **4** and **12** are drastically lowered compared with pure inorganic or even organometallic systems that contain invariably Sn<sup>II</sup> with  $\delta_{\text{IS}} = 3\text{--}4 \text{ mm s}^{-1}$ . Examples of such compounds are the halogenostannates(II) or sandwich complexes like  $[(\eta^5\text{-Cp}^R)_2\text{Sn}^{\text{II}}]$  (R = alkyl).<sup>[41a]</sup> In these compounds the 5s lone pair on tin retains its high  $\sigma$  s character compared with **4** and **12**. Thus, the relatively large values of  $\delta_{\text{IS}}$  for **4** and **12** compared with these compounds seem indicative of some extent of p character in the Sn–Sn (**4**) and Fe–Sn (**12**) bonding induced by rehybridization of the 5s lone pair on Sn.

## Conclusions

We have shown that Fe and Co complexes **10** and **14** containing two (hydrocarbyl)substituted stannylene units :SnR<sub>2</sub> are accessible by different but complementary routes that employ metal vapor chemistry and wet chemical synthesis techniques. Even though the reaction products obtained by both ways differ in their constitution as determined by spectroscopic techniques, they show a similar reactivity towards the nucleophile water. Irreversible water activation occurs with both compounds to give rare cases of hydroxo hydrido complexes, which represent the primary products from such a reaction. Complexes **12** and **15** appear to show strong Sn–H–Fe and Sn–H–Co interactions in solution as judged by <sup>1</sup>H NMR spectroscopy. X-ray crystallography shows them to be isostructural in the solid state. However, a strong Sn–H–Fe interaction in the crystalline state, which was found for **12** in solution, could not be observed in the solid state on the basis of the results of a neutron diffraction study of **12**, which allowed us to characterize the crucial Sn,H,Fe structural parameters unambiguously and characterize **12** as a classical hydride with a normal terminal Fe–H single bond.



## Experimental Section

**General experimental information:** Metal atom reactions were conducted in home-built all-glass static metal vapor reactors based on the design published by Klabunde et al.<sup>18,42</sup> Iron metal was 99% pure. Metal evaporation was performed from resistively heated alumina crucibles (Mathis, CA, USA). In metal vapor reactions, an amount of about 30% of the metal is typically lost because of deposition of metal vapor outside the reaction zone of the metal/toluene condensate. Except for the metal vapor synthesis, all reactions were carried out under an atmosphere of dry nitrogen gas with standard Schlenk techniques. Microanalyses were performed by the microanalytical laboratory of the Chemistry Department of the University/GH-Essen. All solvents were dried appropriately and stored under nitrogen. The NMR spectra were recorded on a Bruker AC 300 and DRX 500 spectrometers (300 and 500 MHz for <sup>1</sup>H, 75.5 and 125.8 MHz for <sup>13</sup>C, 99.36 MHz for <sup>29</sup>Si and 186.5 MHz for <sup>119</sup>Sn) and referenced against the remaining protons of the deuterated solvent used,  $\Xi(^{29}\text{Si}) = 19.867184$  MHz for  $\delta(^{29}\text{Si})(\text{Me}_4\text{Si}) = 0$ , and  $\Xi(^{119}\text{Sn}) = 37.290665$  MHz for  $\delta(^{119}\text{Sn})(\text{Me}_4\text{Sn}) = 0$ . In the case of the <sup>119</sup>Sn NMR experiments, the approximate range of the <sup>119</sup>Sn NMR signals for **12** was first evaluated by heteronuclear <sup>1</sup>H[<sup>119</sup>Sn] double resonance experiments. NMR samples were prepared by vacuum transfer of predried, degassed solvents onto the appropriate amount of solid sample, followed by flame sealing of the NMR tube. MS spectra were recorded on a MAT 8200 instrument under standard conditions (EI, 70 eV) with the fractional sublimation technique for compound inlet. IR spectra were recorded in KBr with a Nicolet 7109 FT- instrument.

### Synthetic procedures:

**Metal vapor synthesis of [( $\eta^6$ -toluene)Fe–Sn{CH(SiMe<sub>3</sub>)<sub>2</sub>}]<sub>2</sub> (**10**):** Iron vapor (2 g, 25 mmol) was codeposited with an excess of toluene (150 mL) at –196 °C over 4 h at 10<sup>–3</sup> Torr. After the reactor had been back-filled with N<sub>2</sub> to ambient pressure, the deep brown solution was filtered through a bed of Celite under a N<sub>2</sub> atmosphere at –78 °C to remove any excess of iron metal. Sn{CH(SiMe<sub>3</sub>)<sub>2</sub>}]<sub>2</sub> (**4**) (1.5 g, 1.7 mmol) dissolved in diethyl ether (20 mL) was added to this solution, causing a color change to intense green after 30 min of stirring at –78 °C. After the mixture had been warmed to room temperature, all the volatile components were removed under vacuum and an oily, greenish brown residue was crystallized from diethyl ether at –78 °C to give **10** as a microcrystalline, green solid in 36% yield. Compound **10** is stable under nitrogen at room temperature for months. MS (EI, 70 eV,  $T_{\text{vap}} = 120$  °C):  $m/z$  (%): decomposition; <sup>1</sup>H NMR ([D<sub>6</sub>]benzene, 27 °C):  $\delta = 59.7$  (s,  $\nu_{1/2} = 203$  Hz, 1H; CH-tol), 45.2 (s,  $\nu_{1/2} = 260$  Hz, 2H; CH-tol), 26.2 (s,  $\nu_{1/2} = 307$  Hz, 2H; CH-tol), 3.3 (s, 3H; CH<sub>3</sub>-tol), 1.1 (s, 36H; SiMe<sub>3</sub>). Various attempts to obtain satisfactory elemental analysis for **10** were unsuccessful because of its high sensitivity to air and moisture.

**Synthesis of [( $\eta^6$ -C<sub>7</sub>H<sub>8</sub>)(OH)(H)Fe–{Sn[CH(SiMe<sub>3</sub>)<sub>2</sub>]}<sub>2</sub>] (**12**) by reaction of [( $\eta^6$ -toluene)Fe–Sn{CH(SiMe<sub>3</sub>)<sub>2</sub>}]<sub>2</sub> (**10**) with H<sub>2</sub>O:** Synthesis of **12** was performed in a one-pot procedure. Compound **4** (1.5 g, 2.67 mmol) dissolved in toluene (10 mL) was added to a deep brown solution of **10** in toluene (150 mL), which had been synthesized by cocondensation of Fe metal (2.0 g) and toluene (150 mL) as described above. The resulting deep green solution was stirred for 2 h at –50 °C, after which H<sub>2</sub>O (2 mL, 0.1 mmol) was added in one batch. During warm-up to room temperature, the color of this solution slowly changed to bright red. Stirring of this solution was continued at room temperature for 2 h. After removal of all the volatile components, the solid residue was dissolved in diethyl ether and filtered, and some CH<sub>3</sub>CN was then added. Cooling of this solution to –30 °C afforded brick-red, rectangular crystals (up to 3 mm large) of **12** (2.04 g, 2.0 mmol, 73.6%). MS (EI, 70 eV,  $T_{\text{vap}} = 140$  °C):  $m/z$  (%): 948 [[Sn{CH(SiMe<sub>3</sub>)<sub>2</sub>}]<sub>2</sub>(tol)Fe–HOH]<sup>+</sup> (1), 604 [Sn{CH(SiMe<sub>3</sub>)<sub>2</sub>}(tol)Fe–H–OH]<sup>+</sup> (2), 586 [Sn{CH(SiMe<sub>3</sub>)<sub>2</sub>}(tol)Fe–H]<sup>+</sup> (2), 494 [Sn{CH(SiMe<sub>3</sub>)<sub>2</sub>FeH]<sup>+</sup> (15), 438 [Sn{CH(SiMe<sub>3</sub>)<sub>2</sub>}]<sup>+</sup> (15); <sup>1</sup>H NMR ([D<sub>6</sub>]benzene, 27 °C):  $\delta = 5.51$  (s,  $\nu_{1/2} = 20.3$  Hz, 2H; *m*-CH, tol), 5.38 (dd, 1H; *p*-CH, tol), 4.55 (s,  $\nu_{1/2} = 20.5$  Hz, 2H; *o*-CH, tol), 2.31 (s, 3H; CH<sub>3</sub>-tol), 1.70 (s,  $\nu_{1/2} = 7.2$  Hz,  $^2J(\text{OH}, ^{117/119}\text{Sn}) = 13$  Hz, 1H; OH), 0.45 (s, 18H; SiMe<sub>3</sub>), 0.42 (s, 18H; SiMe<sub>3</sub>), 0.32 (s, 18H; SiMe<sub>3</sub>), 0.31 (s, 18H; SiMe<sub>3</sub>), –13.42 (s,  $\nu_{1/2} = 27$  Hz,  $J(^{119}\text{Sn}, \text{H}, \text{Fe}) = 640 \pm 30$  Hz, 1H); <sup>13</sup>C NMR [<sup>1</sup>H] ([D<sub>6</sub>]benzene, 27 °C):  $\delta = 100.4$  (s, C<sub>ipso</sub>, tol), 83.7 (s, *o*-CH, tol), 82.1 (s, *p*-CH, tol), 77.8 (s, *m*-CH, tol), 22.4, 22.2 (s, Sn–CH), 22.3 (s, C–CH<sub>3</sub>), 5.8 (s,

SiMe<sub>3</sub>), 5.3 (s, SiMe<sub>3</sub>), 5.0 (s, SiMe<sub>3</sub>); <sup>29</sup>Si and <sup>119</sup>Sn NMR, see text; C<sub>33</sub>H<sub>88</sub>OFeSi<sub>8</sub>Sn: calcd C 40.36, H 8.33; found C 40.64, H 8.40.

**Synthesis of [( $\eta^5$ -Cp)(OH)(H)Co–{Sn[CH(SiMe<sub>3</sub>)<sub>2</sub>]}<sub>2</sub>] (**15**) by reaction of [( $\eta^5$ -Cp)( $\eta^2$ -ethene)Co–Sn{CH(SiMe<sub>3</sub>)<sub>2</sub>}]<sub>2</sub> (**14**) with H<sub>2</sub>O:** H<sub>2</sub>O (0.5 mL) suspended in diethyl ether (10 mL) was added at room temperature to a purple solution of **14** (410 mg, 2.27 mmol) in diethyl ether (50 mL), whereupon the color of the solution changed to reddish brown after a few minutes. After 4 h of additional stirring, all the volatile components were removed under vacuum, and the solid residue was dissolved in diethyl ether/acetonitrile (5:1) and then filtered. Cooling of the bright red, clear solution afforded **15** as red crystals (1.37 mmol, 60.3%). MS (EI, 70 eV,  $T_{\text{vap}} = 130$  °C):  $m/z$  (%): 1018 [ $M^+$ ] (5), 857 [ $M^+ - \text{CH}(\text{SiMe}_3)_2 - 2\text{H}$ ] (5); IR (KBr):  $\tilde{\nu} = 3616$  (O–H); 2950, 2898, 1406, 840 (all TMS); 1250, 1108, 1011, 973, 797, 766 (all Cp); <sup>1</sup>H NMR ([D<sub>6</sub>]benzene, 27 °C):  $\delta = 4.67$  (s, 5H; Cp), 1.63 (br. s, 1H), 0.58 (s, 4H; Sn–CH), 0.42 (s, 18H; SiMe<sub>3</sub>), 0.38 (s, 18H; SiMe<sub>3</sub>), 0.27 (s, 36H; SiMe<sub>3</sub>), –17.57 (s,  $J(^{119}\text{Sn}, \text{H}, \text{Co}) = 539 \pm 20$  Hz, 1H; [Co–H]); <sup>13</sup>C NMR [<sup>1</sup>H] ([D<sub>6</sub>]benzene, 27 °C):  $\delta = 78.7$  (s,  $^2J(^{119}\text{Sn}, \text{C}) = 6.8$  Hz; Cp), 22.2 (s, CH), 5.6 (s,  $^3J(^{119}\text{Sn}, \text{C}) = 12.4$  Hz; SiMe<sub>3</sub>), 5.2 (s,  $^3J(^{119}\text{Sn}, \text{C}) = 13.8$  Hz; SiMe<sub>3</sub>), 4.6 (s, SiMe<sub>3</sub>); C<sub>33</sub>H<sub>83</sub>CoOSi<sub>8</sub>Sn<sub>2</sub>: calcd C 38.97, H 8.23; found C 39.11, H 8.31.

**Synthesis of [( $\eta^5$ -Cp)(OD)(D)Co–{Sn[CH(SiMe<sub>3</sub>)<sub>2</sub>]}<sub>2</sub>] [**D**]**15**:** [**D**]**15** was synthesized in a similar manner to **11** but with D<sub>2</sub>O instead of H<sub>2</sub>O. <sup>2</sup>H NMR ([D<sub>6</sub>]benzene, 27 °C):  $\delta = -17.44$  (s, 1D; [Co–D]), 1.51 (s, 1D; OD), both signals display no detectable <sup>119</sup>Sn coupling; IR (KBr):  $\tilde{\nu}(\text{O}–\text{D})$ , see text.

## Acknowledgements

This work was supported by the Deutsche Forschungsgemeinschaft (Heisenberg fellowship to J.J.S. and grants SCHN 375/3-1 and 3-2), by the Fonds der Chemischen Industrie, and by NSF grant CHE-98-16294 (R.B.). We thank Dr. D. Stöckigt and Dr. K. Seevogel and co-workers (MPI für Kohlenforschung, Mülheim) for recording MS and IR spectra.

- [1] a) P. J. Davidson, M. F. Lappert, *J. Chem. Soc. Chem. Commun.* **1973**, 317; b) J. D. Cotton, P. J. Davidson, D. E. Goldberg, M. F. Lappert, K. M. Thomas, *J. Chem. Soc. Chem. Commun.* **1974**, 893; c) P. J. Davidson, D. H. Harris, M. F. Lappert, *J. Chem. Soc. Dalton Trans.* **1976**, 2268; d) J. D. Cotton, P. J. Davidson, M. F. Lappert, *J. Chem. Soc. Dalton Trans.* **1976**, 2275; e) M. F. Lappert, R. S. Rowe, *Coord. Chem. Rev.* **1990**, *100*, 267; f) P. B. Hitchcock, M. F. Lappert, S. A. Thomas, A. J. Thorne, *J. Organomet. Chem.* **1986**, *315*, 27; g) P. B. Hitchcock, M. F. Lappert, M. C. Misra, *J. Chem. Soc. Chem. Commun.* **1985**, 863; h) P. B. Hitchcock, M. F. Lappert, S. A. Thomas, A. J. Thorne, A. J. Carthy, N. J. Taylor, *J. Organomet. Chem.* **1986**, *315*, 27; i) M. Weidenbruch, A. Stilter, K. Peters, H. G. von Schnering, *Chem. Ber.* **1996**, *129*, 1565; j) M. Weidenbruch, A. Stilter, K. Peters, H. G. von Schnering, *Z. Anorg. Allg. Chem.* **1996**, *14*, 365; k) M. Weidenbruch, A. Stilter, W. Saack, K. Peters, H. G. von Schnering, *J. Organomet. Chem.* **1998**, *560*, 125; l) K. W. Klinkhammer, W. Schwarz, *Angew. Chem.* **1995**, *107*, 1448; *Angew. Chem. Int. Ed. Engl.* **1995**, *34*, 1334; m) K. W. Klinkhammer, T. F. Fässler, H. Grützmacher, *Angew. Chem.* **1998**, *110*, 114; *Angew. Chem. Int. Ed.* **1998**, *37*, 124; n) U. Layh, H. Pritzkow, H. Grützmacher, *J. Chem. Soc. Chem. Commun.* **1992**, 260; o) D. E. Goldberg, D. H. Harris, M. F. Lappert, K. M. Thomas, *J. Chem. Soc. Chem. Commun.* **1976**, 261; p) M. Weidenbruch, H. Kilian, K. Peters, H. G. von Schnering, H. Marsmann, *Chem. Ber.* **1995**, *128*, 983; q) for a recent review dealing with **4**, the prototype of a bis-silylstannylene :SnR<sub>2</sub>, see P. P. Power, *J. Chem. Soc. Dalton Trans.* **1998**, 2939; r) M. Veith, L. Stahl, V. Huch, *J. Chem. Soc. Chem. Commun.* **1990**, 359; s) M. Veith, *Angew. Chem.* **1975**, *87*, 287; *Angew. Chem. Int. Ed. Engl.* **1975**, *14*, 263; *Z. Naturforsch. Teil B*, **1978**, *33*, 7; t) J. J. Schneider, N. Czap, *J. Chem. Soc. Dalton Trans.* **1999**, 595; u) a monomer–dimer equilibrium has been firmly established for **4**, see K. W. Zilm, G. A. Lawless, R. M. Merrill, J. M. Miller, G. G. Webb, *J. Am. Chem. Soc.* **1987**, *109*, 7236; S. Masamune, Y. Eriyama, T. Kawase, *Angew. Chem.* **1987**, *99*, 601; *Angew. Chem. Int. Ed. Engl.* **1987**, *26*, 584.
- [2] The term *hydrocarbyl* or *silyl* indicates that no O or N donor atom is directly bonded to tin in :SnR<sub>2</sub>.

- [3] a) C. Pluta, K. R. Pörschke, R. Mynott, P. Betz, C. Krüger, *Chem. Ber.* **1991**, *124*, 132; b) J. Krause, C. Pluta, K. R. Pörschke, R. Goddard, *J. Chem. Soc. Chem. Commun.* **1993**, 1254; c) J. Krause, K. H. Haack, K.-R. Pörschke, B. Gabor, R. Goddard, C. Pluta, K. Seevogel, *J. Am. Chem. Soc.* **1996**, *118*, 804.
- [4] a) J. J. Schneider, N. Czap, D. Bläser, R. Boese, *J. Am. Chem. Soc.* **1999**, *121*, 1409; b) J. J. Schneider, J. Hagen, D. Bläser, R. Boese, *Angew. Chem.* **1997**, *109*, 771; *Angew. Chem. Int. Ed. Engl.* **1997**, *36*, 739; c) J. J. Schneider, N. Czap, *J. Chem. Soc. Dalton Trans.* **1999**, 595.
- [5] a) R. Dorta, A. Togni, *Organometallics* **1998**, *17*, 3423; b) D. Milstein, J. C. Calabrese, I. D. Williams, *J. Am. Chem. Soc.* **1986**, *108*, 6387; c) O. Blum, D. Milstein, *Angew. Chem.* **1995**, *107*, 210; *Angew. Chem. Int. Ed. Engl.* **1995**, *34*, 229; d) F. T. Lapido, M. Kooti, J. S. Merola, *Inorg. Chem.* **1993**, *32*, 1681; e) M. J. Burns, M. G. Fickes, J. F. Hartwig, F. Hollander, R. G. Bergman, *J. Am. Chem. Soc.* **1993**, *115*, 5875; f) D. J. Cole-Hamilton, G. Wilkinson, *Nouv. J. Chim.* **1977**, *1*, 141; g) K. Tani, A. Iseki, T. Yamagata, *Angew. Chem.* **1998**, *110*, 3590; *Angew. Chem. Int. Ed.* **1998**, *37*, 3381.
- [6] a) R. C. Steven, R. Bau, D. Milstein, O. Blum, T. F. Koetzle, *J. Chem. Soc. Dalton Trans.* **1990**, 1429; b) K. B. Renkema, J. C. Huffman, K. O. Caulton, *Polyhedron* **1999**, *18*, 2575.
- [7] a) C. Elschenbroich, A. Salzer, *Organometallics*, 2. Auflage, Teubner, **1988**; C. Elschenbroich, A. Salzer, *Organometallics*, 2nd ed, VCH, Weinheim, **1992**; b) A. G. Davies, *Organotin Chemistry*, VCH, Weinheim, **1997**.
- [8] K. J. Klabunde, Y. X. Li, B. J. Tan, *Chem. Mater.* **1991**, *3*, 30.
- [9] a) L. K. Beard, Jr., M. P. Silvon, P. S. Skell, *J. Organomet. Chem.* **1981**, *209*, 245; b) G. A. Ozin, C. G. Francis, H. X. Huber, M. Andrews, L. Nazar, *J. Am. Chem. Soc.* **1981**, *103*, 2453; c) H. F. Efer, D. E. Tevault, W. B. Fox, R. R. Smardzewski, *J. Organomet. Chem.* **1978**, *146*, 45.
- [10] a) U. Zenneck, *Angew. Chem.* **1990**, *102*, 171; *Angew. Chem. Int. Ed. Engl.* **1990**, *29*, 126; b) J. J. Schneider, U. Specht, R. Goddard, C. Krüger, J. Ensling, P. Gütlich, *Chem. Ber.* **1995**, *128*, 941; c) J. J. Schneider in *Chemistry under Extreme or Non-Classical Conditions* (Eds.: R. van Eldik, C. D. Hubbard), Wiley-Spektrum, Heidelberg, **1996**.
- [11] J. J. Schneider, J. Hagen, D. Bläser, R. Boese, F. Fabrizi de Biani, P. Zanello, C. Krüger, *Eur. J. Inorg. Chem.* in press.
- [12] F. Schager, K. Seevogel, K.-R. Pörschke, M. Kessler, C. Krüger, *J. Am. Chem. Soc.* **1996**, *118*, 13075.
- [13] F. Schager, R. Goddard, K. Seevogel, K. R. Pörschke, *Organometallics* **1998**, *17*, 1546.
- [14] a) H. P. Fritz, H. J. Keller, K. E. Schwarzans, *Z. Naturforsch. B* **1968**, *23*, 298; b) H. J. Keller, K. E. Schwarzans, *Angew. Chem.* **1970**, *82*, 227; *Angew. Chem. Int. Ed. Engl.* **1970**, *9*, 196.
- [15] C. Elschenbroich, F. Gerson, *J. Organomet. Chem.* **1973**, *49*, 445.
- [16] J. J. Schneider, U. Specht, R. Goddard, C. Krüger, J. Ensling, P. Gütlich, *Chem. Ber.* **1995**, *128*, 941.
- [17] S. D. Ittel, C. A. Tolman, *J. Organomet. Chem.* **1979**, *172*, C47.
- [18] U. Zenneck, W. Franck, *Angew. Chem.* **1986**, *98*, 806; *Angew. Chem. Int. Ed. Engl.* **1986**, *25*, 831.
- [19] a) V. S. Asirvatham, Z. Yao, K. J. Klabunde, *J. Am. Chem. Soc.* **1994**, *116*, 5493; b) Z. Yao, K. J. Klabunde, A. S. Asirvatham, *Inorg. Chem.* **1995**, *34*, 5289.
- [20] Z. Yao, K. J. Klabunde, *Organometallics* **1995**, *14*, 5013.
- [21] U. Schubert, *Adv. Organomet. Chem.* **1990**, *30*, 151.
- [22] A. G. Davies, P. J. Smith in *Comprehensive Organometallic Chemistry*, Vol. 2 (Eds.: G. Wilkinson, F. G. A. Stone, E. Abel), Pergamon, Oxford, **1982**, p. 586.
- [23] U. Schubert, E. Kunz, B. Harkers, J. Willnecker, J. Meyer, *J. Am. Chem. Soc.* **1989**, *111*, 2572.
- [24] H. Piana, U. Kirchgäßner, U. Schubert, *Chem. Ber.* **1991**, *124*, 743.
- [25] U. Schubert, S. Gilbert, S. Mock, *Chem. Ber.* **1992**, *125*, 835.
- [26] A. Khaleel, K. J. Klabunde, A. Johnson, *J. Organomet. Chem.* **1999**, *572*, 1999.
- [27] M. Akita, T. Oku, M. Tanaka, Y. Moro-oka, *Organometallics* **1991**, *10*, 3080.
- [28] P. Legzdins, M. Shaw, R. J. Batchelor, F. W. B. Einstein, *Organometallics* **1995**, *14*, 4721.
- [29] A rather small value of  $^2J(\text{Sn}, \text{H}) = 23.7 \text{ Hz}$  was found in  $[(\text{Cp})\text{Cr}(\text{NO})(\text{PPh}_3)(\text{H})\text{SnPh}_3]$ .<sup>[28]</sup> The authors assume the "existence of some three-center, two-electron Sn-H-Cr bonding, analogous to that for Schubert's  $[(\eta^5\text{-MeC}_5\text{H}_4)(\text{CO})_2\text{Mn}(\text{H})\text{SnPh}_3]$ ." Their assumption was solely based on the X-ray crystallographic data, despite the experimental result that the hydride ligand "was only poorly defined" in that work.
- [30] A. N. Protsky, B. M. Bulychev, G. Solovchik, V. K. Belskey, *Inorg. Chim. Acta* **1986**, *115*, 121.
- [31] B. Wrackmeyer, *Annu. Rep. NMR Spectrosc.* **1999**, *38*, in press.
- [32] X-ray crystallographic investigations of **12** and **15**. Compound **12**:  $\text{C}_{35}\text{H}_{85}\text{FeOSi}_8\text{Sn}_2$ ,  $M_r = 1039.98$ ,  $a = 13.7542(8)$ ,  $b = 17.7220(10)$ ,  $c = 23.6570(10) \text{ \AA}$ ,  $\beta = 104.1050(10)^\circ$ ,  $V = 5592.6 \text{ \AA}^3$ ,  $Z = 4$ , monoclinic  $P2_1/n$  (no. 14),  $\rho_{\text{calcd}} = 1.235 \text{ Mg m}^{-3}$ ,  $\mu(\text{MoK}\alpha) = 1.336 \text{ mm}^{-1}$  at  $T = 100 \text{ K}$ . Diffraction data from a crystal with dimensions of  $0.53 \times 0.46 \times 0.35 \text{ mm}$  were collected on a Siemens SMART-CCD area detector system equipped with a sealed X-ray tube, graphite monochromator ( $\lambda = 0.71069 \text{ \AA}$ ), and a liquid nitrogen gas stream cooling device. A total of 22001 reflections with  $\theta_{\text{max}} = 23.25^\circ$  resulted in 8005 unique data ( $R_{\text{int}} = 0.078$ ) with 7176 reflections having intensities  $> 2\sigma(I)$  uncorrected for absorption. The structure was solved by the heavy atom method (SHELXL-86)<sup>[42]</sup> followed by full-matrix least-squares refinement of 427 parameters against  $F^2$  for all reflections, as implemented in the program SHELXL-93.<sup>[43]</sup> Hydrogen atoms were placed at idealized positions and refinement converged at  $R = 0.038$  and  $wR^2 = 0.111$ , highest peak and lowest trough of residual electron density  $1.7$  and  $-0.8 \text{ e \AA}^{-3}$ . Compound **15**:  $\text{C}_{33}\text{H}_{82}\text{CoOSi}_8\text{Sn}_2$ ,  $M_r = 1016.02$ ,  $a = 18.452(3)$ ,  $b = 11.9089(14)$ ,  $c = 24.861(4) \text{ \AA}$ ,  $\beta = 104.752(15)^\circ$ ,  $V = 5273.4(14) \text{ \AA}^3$ ,  $Z = 4$ , monoclinic  $P2_1/a$  (no. 13),  $\rho_{\text{calcd}} = 1.280 \text{ Mg m}^{-3}$ ,  $\mu(\text{MoK}\alpha) = 1.454 \text{ mm}^{-1}$  at  $T = 293 \text{ K}$ . Diffraction data from a crystal with dimensions of  $0.62 \times 0.32 \times 0.15 \text{ mm}$  were collected on an Enraf-Nonius CAD4 goniometer equipped with a sealed X-ray tube and graphite monochromator ( $\lambda = 0.71069 \text{ \AA}$ ), which gave 12019 unique reflections with  $\theta_{\text{max}} = 27.42^\circ$  and 8552 reflections of intensities  $> 2\sigma(I)$  not corrected for absorption. The structure was solved by the heavy atom method<sup>[42]</sup> followed by full-matrix least-squares refinement of 410 parameters against  $F^2$  for all reflections, as implemented.<sup>[43]</sup> Hydrogen atoms were placed at idealised positions and refinement converged at  $R = 0.0431$  and  $wR^2 = 0.1539$ , highest peak and lowest hole of residual electron density  $1.071$  and  $-1.577 \text{ e \AA}^{-3}$ .  $H(100)$  was found but not refined because of the unrealistic  $U$  values obtained during the refinement procedure. Crystallographic data (excluding structure factors) for the structures reported in this paper have been deposited with the Cambridge Crystallographic Data Centre as supplementary publication no. CCDC-117900 (**12**) and 117901 (**15**). Copies of the data can be obtained free of charge on application to CCDC, 12 Union Road, Cambridge CB2 1EZ, UK (fax: (+44) 1223-336-033; e-mail: deposit@ccdc.cam.ac.uk). Neutron diffraction investigation of **12**: diffraction data were collected on a single crystal at the Institut Laue-Langevin in Grenoble on instrument D-19 with a  $4^\circ \times 64^\circ$  area detector.<sup>[44]</sup> A red-brown crystal of **12** with an approximately cubic shape ( $1.5 \times 1.5 \times 1.5 \text{ mm}$ ) was sealed with epoxy in an inert-atmosphere chamber, mounted on a vanadium pin and covered with a quartz tube inside a Displex cryorefrigerator.<sup>[45]</sup> The data collected at  $20 \text{ K}$  with neutrons of wavelength  $1.5345(1) \text{ \AA}$  were integrated in three dimensions on the ILL program RETREAT.<sup>[46]</sup> A total of 10723 reflections were merged to give a final data set of 5675 unique reflections ( $R_{\text{merge}} = 0.036$ ) that were used in the subsequent structure analysis. The neutron data set of **12** was phased by the atomic positions of the non-hydrogen atoms from the prior X-ray analysis.<sup>[31]</sup> A series of difference Fourier maps revealed the positions of all the hydrogen atoms in the molecule, and the unique hydride ligand was immediately found to be in an essentially terminal position, but disordered (vide infra). The entire structure analysis was complicated by extensive disorder of the diethyl ether solvate molecule, as well as a 3:1 coupled disorder of the toluene and hydride ligands. Exhaustive least-squares refinement<sup>[43]</sup> of the structure (with the diethyl ether solvate molecule constrained with ideal molecular parameters) resulted in final agreement factors of  $R(F) = 0.078$  for 4860 reflections with  $I > 2\sigma(I)$ , and  $R(F) = 0.091$  for all 5675 reflections. The results of the neutron diffraction analysis are summarized in Table 3, and selected distances and angles in the molecule are given in Table 4.
- [33] R. G. Teller, R. Bau, *Struct. Bonding (Berlin)* **1981**, *44*, 1.
- [34] a) F. Lutz, R. Bau, P. Wu, T. F. Koetzle, C. Krüger, J. J. Schneider, *Inorg. Chem.* **1996**, *35*, 2698; b) J. L. Kersten, A. L. Rheingold, K. H.

- Theopold, C. P. Casey, R. A. Widenhoefer, C. E. C. A. Hop, *Angew. Chem.* **1992**, *104*, 1364; *Angew. Chem. Int. Ed. Engl.* **1992**, *31*, 1341.
- [35] R. Bau, M. H. Drabnis, *Inorg. Chim. Acta*, **1997**, *259*, 27.
- [36] To our knowledge, there have been no reports of accurate measurements of Sn–H distances carried out by neutron diffraction in the solid state thus far. However, reasonable estimates can be obtained by comparison with Si–H distances, which have been well characterized. From the many published<sup>[47]</sup> Si–CH<sub>3</sub> (average 1.876 Å) and Sn–CH<sub>3</sub> (average 2.147 Å) distances, one can estimate the difference between the Si and Sn covalent radii to be 0.27 Å. By combining this number with the Si–H distance of 1.502 Å obtained by neutron diffraction,<sup>[48]</sup> one gets an estimate of 1.77 Å for the Sn–H single bond, which agrees reasonably well with the experimental value of 1.701(5) Å obtained from SnH<sub>4</sub> by electron diffraction.<sup>[49]</sup> The bridging Sn···H (or “agostic”) distance can be similarly estimated from the known Si···H agostic distance of 1.80 Å found in a Si···H–Mn bridged compound.<sup>[50]</sup> Applying the same 0.27 Å correction factor between Si and Sn then yields an estimated 2.07 Å for a Sn···H bridging or agostic interaction.
- [37] Iron and tin Mössbauer measurements of **12**: the <sup>57</sup>Fe Mössbauer spectrum was recorded with a constant-acceleration type Mössbauer spectrometer. The spectrometer was equipped with a 1024-channel analyzer operating in the time scale mode, and a 25 mCi <sup>57</sup>Co/Rh source was employed. The isomer shifts reported here are relative to α-Fe at room temperature. The spectrum was recorded at 100 K by means of a combined He continuous flow/bath cryostat (sample thickness was about 5 mg Fe cm<sup>-2</sup>). The <sup>119</sup>Sn Mössbauer spectrum was taken at 100 K with a <sup>119</sup>Sn source by means of a combined He continuous flow/bath cryostat (Cryovac, Troisdorf) in transmission geometry on a constant acceleration type standard Mössbauer spectrometer (Wissel, Starnberg, Germany). The isomer shifts reported here are relative to CaSnO<sub>3</sub> at room temperature.
- [38] N. N. Greenwood, T. C. Gibb, *Mössbauer Spectroscopy*, Chapman and Hall, London, **1971**.
- [39] J. J. Zuckerman, *J. Organomet. Chem.* **1973**, *49*, 1.
- [40] R. H. Herber, *Progr. Inorg. Chem.* **1967**, *8*, 1.
- [41] a) R. V. Parish in *Mössbauer Spectroscopy Applied to Inorganic Chemistry, Vol. 1* (Ed.: G. J. Long), Plenum Press, New York, **1984**; b) J. D. Cotton, P. J. Davidson, M. F. Lappert, L. K. M. Thomas, J. D. Donaldson, J. Silver, *J. Chem. Soc. Dalton Trans.* **1976**, 261.
- [42] K. J. Klabunde in *Reactive Intermediates* (Ed.: R. Abramovitch), Plenum Press, New York, **1979**.
- [43] a) G. M. Sheldrick, *Acta Crystallogr. Sect. A*, **1990**, *46*, 467; b) G. M. Sheldrick, SHELXL-93, University of Göttingen, Germany, **1993**.
- [44] M. Thomas, R. F. D. Stansfield, M. Berneron, A. Filhol, G. Greenwood, J. Jacobe, D. Feltin, S. A. Mason in *Position-sensitive Detection of Thermal Neutrons* (Eds.: P. Convert, J. B. Forsyth), Academic Press, **1983**, 344.
- [45] J. Archer, M. S. Lehmann, *J. Appl. Crystallogr.* **1986**, *19*, 456.
- [46] C. Wilkinson, H. W. Khamis, R. F. D. Stansfield, G. J. McIntyre, *J. Appl. Crystallogr.* **1988**, *21*, 471.
- [47] The Cambridge Structural Database, **1999**.
- [48] J. A. K. Howard, P. A. Keller, T. Vogt, A. L. Taylor, N. D. Dix, J. L. Spencer, *Acta Crystallogr. Sect. B* **1992**, *48*, 438.
- [49] The Chemical Society, *Tables of Interatomic Distances and Configuration in Molecules and Ions*, Special Publication No. 18, **1965**, p. S12s.
- [50] U. Schubert, K. Ackermann, B. Wörle, *J. Am. Chem. Soc.* **1982**, *104*, 7378.

Received: June 7, 1998 [F1834]